Differential Spatial Representations in Hippocampal CA1 and Subiculum Emerge in Evolved Spiking Neural Networks

Kexin Chen[1], Alexander Johnson[3], Eric O. Scott[4], Xinyun Zou[2],
Kenneth A. De Jong[4], Douglas A. Nitz[3], and Jeffrey L. Krichmar[1,2]

[1]*Department of Cognitive Sciences, University of California, Irvine, Irvine, CA, USA*
[2]*Department of Computer Science, University of California, Irvine, Irvine, CA, USA*
[3]*Department of Cognitive Science, University of California, San Diego, La Jolla, CA, USA*
[4]*Department of Computer Science, George Mason University, Fairfax, VA, USA*
Correspondence Email: kexinc3@uci.edu

***Abstract*—In rodent navigational studies, spatial responses have been identified in both the hippocampal subregion CA1 and the subiculum (SUB), but these two brain regions appear to encode spatial features differently. Place fields of SUB place cells are larger and less specific than CA1. Additionally, SUB neurons exhibit stronger directional modulation for heading and axes of travel. Based on neural and behavioral data recorded as rats perform a navigational task on a "triple-T" maze, we present a spiking neural network modeling framework to replicate response properties observed in the CA1 and SUB. The parameters of Spike Timing Dependent Plasticity and homeostatic scaling (STDP-H) were evolved such that the response of the two different SNNs resembled recordings from CA1 and SUB when rats traversed the triple-T maze. Our results suggest that positional input may be more influential in forming CA1 place cells, while the SUB appears to integrate both allocentric positional information and self-motion cues to encode "kinds of places". Furthermore, our results predict that the different spatial responses in these regions may be due in part to different STDP-H learning parameters. The framework presented here could be used as an automated parameter tuning system for replicating responses in other brain regions.**

I. Introduction

Rodents flexibly and reliably navigate in the world by using a variety of available spatial information. Effective spatial navigation is supported by localizing oneself in the environment, knowing the current direction of movement, and inferring about the progress along routes leading to the destination. Several regions in the rodent brain have been identified as important for spatial navigation, including the hippocampal sub-region CA1 and the subiculum (SUB). Lesions of both regions cause deficits in navigational abilities and a loss of accurate localization ability [1]. On the single cell level, place cells have been identified in both regions [2], [3]. Place cells were shown to signal the allocentric position of the animal during navigational tasks. These cells fire selectively in specific locations in the environment, and the population ensemble activity can be used to decode the animal's movement [4]. However, compared to CA1, SUB place cells showed larger, less specific place fields [5], and exhibit more directional modulation for activity within those fields [3], [6].

A number of computational models have been proposed to explain the emergence of CA1 place cells [7]–[9], but fewer computational studies concern the spatial representations in SUB neurons. As biologically detailed models, Spiking Neural Networks (SNNs) have been used to investigate sensory processing in the brain [10] and to model brain activities [11]. Different methods of optimizing SNNs have also been proposed, such as unsupervised learning with spike timing dependent plasticity (STDP) [12] and evolving the structure of the network [11]. Our method is unique that we evolve the synaptic learning rule in SNNs to map recorded behavioral data to neuronal data.

In this paper, we extend the method of evolving SNNs introduced in [13] to replicate neural dynamics of CA1 and SUB neurons. We use datasets recorded from the CA1 and SUB while rats performed a complex navigational task on a triple-T maze (Fig. 1) [14]. Neural circuits of both regions are modeled with SNNs optimized by evolving spike timing dependent plasticity with homeostatic scaling (STDP-H) parameters using evolutionary algorithms (EAs). In the SNN models, behavioral variables including the allocentric position of the animal and self-motion related variables such as the head direction and linear/angular velocity of the animal serve as the input to the network, and a recurrently connected group of excitatory spiking neurons is tuned to replicate the CA1 and SUB neural activity. Our results suggest that the same spiking neural network modeling framework can be used to model different brain regions related to spatial navigation. In addition, analysis of the connection weights and results from ablation studies are suggestive of how CA1 and SUB integrate sensory information differently to form spatial representations. The CA1 region fires sparsely and less actively with higher spatial information, whereas the SUB is more active and directionally selective. These differences are captured in the connection weights and the evolved STDP-H parameters of these regions.

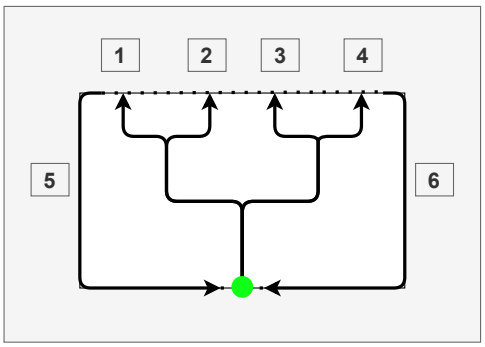

Fig. 1: Schematic drawing of the navigational task. The rat would start from the bottom (indicated by a green dot), take one of the four internal routes (i.e., Routes 1-4) to get to a reward site, and return to the starting point via one of the two return routes (i.e., Routes 5-6). The rats demonstrated remarkable navigation ability and working memory capacity by visiting all four reward sites with minimal repeats.

II. Methods

We took a unique modeling approach of evolving hyper-parameters in spiking neural networks. Spiking neural networks are preferable in this study as they accurately captured the nature of our datasets, which included spike trains that were distributed into spatial bins and processed with a smoothing function [6]. We processed the spike trains in our spiking models following the same procedure to ensure a direct comparison with the recorded data. The models were optimized with an approach combining evolutionary algorithms (EAs) and unsupervised learning using STDP and homeostatic synaptic scaling (STDP-H) [13]. The EAs searched for optimal hyper-parameters for the STDP-H learning rule, without directly updating the connection weights in the network. To ensure the reliability of our modeling and parameter search process, we carried out 5 independent evolutionary runs for each modeled region, each with a population size of 15 individual networks that underwent 50 generations of EA.

All simulations were performed with the CARLsim 4 spiking neural network simulator [15]. CARLsim 4 includes a parameter tuning interface (PTI) that links to an evolutionary computation library called ECJ [16].

A. Network Model

The network model contained 1282 neurons in total: 640 excitatory neurons modeled as regular spiking (RS) Izhikevich spiking neurons, 160 inhibitory neurons modeled as fast spiking (FS) Izhikevich spiking neurons [17], and 482 input neurons modeled as Poisson spike generators. The input layer contained four types of behavioral inputs: 450 neurons for allocentric position (Pos), 12 neurons for angular velocity (AV), 12 neurons for linear velocity (LV), and 8 neurons for head direction (HD). Each input group was connected to both the excitatory and inhibitory groups. The inhibitory neuron group provided feed-forward inhibition to the excitatory neuron group, while the excitatory neuron group had recurrent excitatory connections within its own group. Neuron groups were sparsely connected with a probability of 0.1 (Fig. 2).

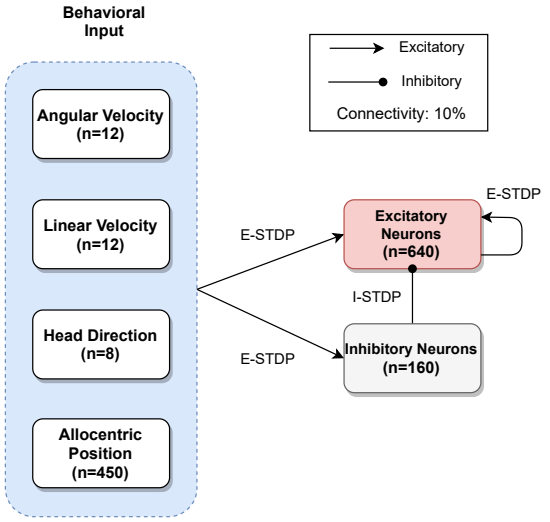

Fig. 2: Network architecture. This network contains four input neuron groups, representing four types of behavioral variables: angular velocity (AV), linear velocity (LV), head direction (HD), and allocentric position (Pos) of the rat. The input neuron groups are connected to an excitatory neuron group and an inhibitory neuron group. Neurons within and between groups have a connection probability of 0.1.

Input streams to the SNNs represented the kinds of information processed by connected regions. For example the hippocampal sub-region CA3 provides positional information [18], the medial entorhinal cortex (MEC) provides velocity related information [19], and the anterior thalamic nucleus (ATN) provides movement and head direction related information [20], [21] to CA1 and SUB. We created the tuning curves for each type of input streams following the same fashion as in [13]. Parameter values were set to allow the tuning curves to cover the entire value range in our datasets and elicit varying neuronal responses. The analog response from the tuning curves was converted into spike trains using a Poisson spike generator.

B. Evolutionary Computation

Instead of directly evolving the connection weights, we employed a "learning to learn" paradigm and evolved a total of 20 hyper-parameters in our network. The hyper-parameters in the network fell into 3 categories: (1) Parameters of the STDP learning rule, which included the amplitude parameters $A+$ and $A-$, and the time decay constants $\tau+$ and $\tau-$. Optimal values for these parameters were searched for the Excitatory-STDP that projected into both the excitatory (EE) and inhibitory (EI) neuron groups, and the Inhibitory-STDP that projected into the excitatory (IE) neuron group. (2) Parameters of the homeostatic synaptic scaling rule that were applied to the excitatory and inhibitory neuron groups, which included the target firing rate R_{target} and the time scale

parameter T. (3) The maximum connection weights for the inter-group connections (i.e., Inp $\rightarrow$ Exc, Inp $\rightarrow$ Inh, Exc $\rightarrow$ Exc, Inh $\rightarrow$ Exc).

Models were optimized through 50 generations of EA. In the first generation, the EA initialized 15 networks, each of which went through a training and testing phase and obtained a fitness score. Parameters of the best performing 3 networks were then used to generate a new generation of 15 network individuals using the (μ, λ) Evolutionary Strategy (ES) [16].

C. Training and Testing of the Model

We used a subset of the data in [14], which included 5430 trials from 32 recording sessions for CA1, and 5908 trials from 49 recordings for SUB. Each trial contained neuronal activity recorded from one brain region and behavioral variables of the animal as it traversed one of the six routes of the maze shown in Fig. 1. For both CA1 and SUB datasets, we shuffled the data based on trials and split them in half to create a pool of training data and a pool of testing data.

In each EA generation, a population of networks with different hyper-parameters went through a training and a testing phase, and the fitness scores of the networks were evaluated by the EA to generate the hyper-parameters for the next generation. The training and testing datasets each consisting of 600 trials (i.e., 100 trials for each route) were re-sampled every generation from the training and testing data pools respectively. In the training phase, behavioral data were fed into the network and STDP-H learned associations between neurons and stabilized network activity. STDP updated the connection weights based on the temporal distance of pre- and post-synaptic spikes, and homeostatic scaling modified the weights in a multiplicative manner based on the post-synaptic firing rate [22]. During testing, we disabled synaptic plasticity and froze the connection weights. We presented the network with different behavioral data from the testing data pool while recording neural activity. To determine how well the simulated neurons resembled the experimentally observed neurons, a Pearson correlation coefficient, ρ, was computed between the mean firing rate of excitatory neuron activity in the SNN and experimentally observed neurons. Using a greedy approach, we determined a match between a simulated neuron and an experimentally observed neuron based on the highest correlation value and each neuron could only be matched once. After all experimentally observed neurons found a match, a fitness value of the network was calculated by summing the ρ values of all matched neuron pairs:

$$y = \sum_{i}^{N} \rho(\bar{R}^i_{real}, \bar{R}^i_{match}) - L \tag{1}$$

where L was a penalty for unrealistically high firing rates, which only applied when the maximum mean firing rate of one of the excitatory neurons R_{exc} exceeded the threshold firing rate $R_t = 100$ Hz:

$$L = \begin{cases} max(\bar{R}_{exc}) - R_t & \text{, if } \quad max(\bar{R}_{exc}) > R_t \\ 0 & \text{, } otherwise \end{cases}, \tag{2}$$

Although only a subset of neurons in the excitatory neuron group were matched to the recorded neurons, the entire neuron group was intended to model a larger population of CA1 and SUB neurons. Neurons that were not explicitly matched to the recorded neurons were expected to have similar response properties as those that were explicitly matched.

D. Positional Reconstruction Matrix

Population analysis of the neuronal activity was conducted by comparing the positional reconstruction matrices of the simulated neurons in the models and experimentally observed neurons in our datasets [23] . We concatenated the neuronal activity in every positional bin of all six routes and computed mean firing rate vectors for every neuron based on odd and even trials. We obtained mean rate matrices $R_{odd} \in \mathbb{R}^{n \times m}$ and $R_{even} \in \mathbb{R}^{n \times m}$ for the entire neuron population, where n represented the number of neurons in the population, and m represented the number of positional bins in the maze. Each column in the matrix represented the population activity in a specific positional bin. We then computed the positional reconstruction matrix based on the columns of the odd trial ensemble rate matrix and the even trial one:

$$M = \rho(R_{odd}, R_{even}), \quad M \in \mathbb{R}^{m \times m} \tag{3}$$

where $\rho(\cdot)$ computes the Pearson correlation coefficient.

Comparing the positional reconstruction matrix of simulated neurons and experimentally recorded neurons allowed us to gauge how well the response properties of simulated neurons resembled those of recorded neurons. A similarity score was obtained by converting the matrices into column vectors and correlating the two vectors:

$$g = \rho(M_{simulated}, M_{recorded}), g \in \mathbb{R}^{1 \times 1} \tag{4}$$

Different from the fitness function (Equation 1), this measurement took into account neurons that were not explicitly matched to the recorded neurons, and thus also tested whether the learned response properties generalized to the entire simulated neuron population.

III. Results

A. Evolved Networks Captured Properties of Both Regions

SNN models were optimized such that a subset of the excitatory neurons had firing patterns aligned with those of experimentally recorded neurons (295 neurons in the CA1 dataset, and 382 neurons in the SUB dataset). As described in Section II-C, fitness function of the network was defined to be the sum of pairwise correlation values of all simulated-recorded neuron pairs, with a penalty for high firing rates of the simulated neurons (Equation 1). The highest fitness scores that could be achieved by the CA1 and SUB models were 295 and 382 respectively.

We conducted 5 evolutionary runs for each model. With a population of 15 individual networks, the best fitness score in the first generation averaged to be 140.44 for the CA1 model and 136.83 for the SUB model. As shown in Fig. 3, by 50 generations, the networks achieved an averaged fitness score of 186.97 for the CA1 model, and 213.48 for the SUB model, corresponding to a mean Pearson's ρ value of 0.63 and 0.56 respectively (normalized to the number of recorded neurons in each brain region). The fitness scores were comparable to those reported in [13]. These scores showed that the firing patterns of experimentally observed neurons were captured by a subset of neurons in the excitatory neuron group. The networks also showed a generalization ability, as excitatory neurons that were not explicitly matched to the recorded neurons also showed response properties similar to those observed in CA1 and SUB.

Similar to rodent recordings [6], [14], we observed spatially selective place cell responses in the simulated CA1 and directionally modulated responses along maze axes in the simulated SUB (Fig. 4). Simulated neurons in the CA1 model were mostly quiet in other positions, and had lower firing rates than the simulated SUB. Simulated neurons in the SUB had higher firing rates and responded to multiple locations. As has been observed in the rat, some of the SUB neurons encoded analogous spaces and were sensitive to the direction of travel.

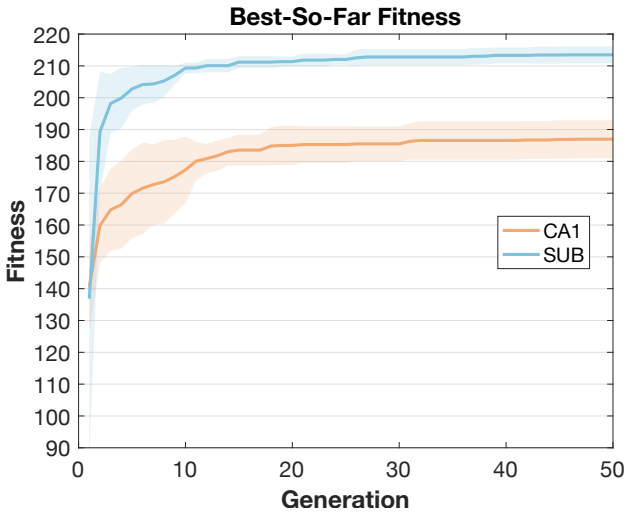

Fig. 3: Best-so-far fitness scores over 50 generations for the CA1 and SUB models. Solid lines show the mean and shaded areas show the standard deviation of 5 runs. At generation 50, the CA1 model reached a mean fitness score of 186.97 and the SUB model had a mean score of 213.48, corresponding to a mean Pearson's ρ value of 0.63 and 0.56 respectively.

After training, the distribution of weights reflected the function of the brain region. Fig. 5 shows the histogram of connection weights from the input variables to the excitatory neuron groups. In the CA1 model (Fig. 5, top row), connection weights showed a U-shape distribution pattern. The weight values clustered at the limiting values (i.e. 0 and maximum weight), with more values near 0 for AV, LV, and HD, and more values near the maximum weight for Pos. This reflects

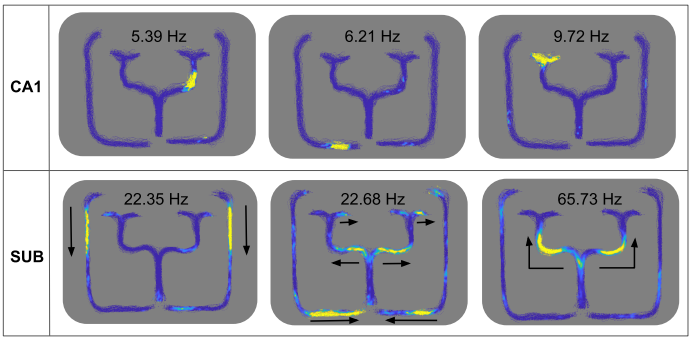

Fig. 4: Examples of representative excitatory neurons in the CA1 and SUB models. Each firing rate map is labeled with the maximum firing rate of the neuron. Model units exhibit differential spatial representations: CA1 model units show single place fields, while the SUB model units respond to multiple locations that are analogous with respect to maze structures. The first and third SUB units show examples of analogy cells, and the second SUB unit shows an example of an axis-tuned cell. Arrows denote the direction of travel.

the place encoding observed in this region. In contrast, a large proportion of connection weights in the SUB model (Fig. 5, bottom row) clustered near the maximum weight, with all four types of input variables showing a similar distribution. The responsiveness of SUB neurons, on average, to a broader set of positional, directional, and self-motion input types may be key to generation of firing fields in multiple locations that are analogous in terms of the direction of travel and location within topologically similar routes

Interestingly, the STDP parameters evolved to support these differential responses. Fig. 6 shows the evolved STDP curves for the two modeled brain regions. Compared to the SUB model, the CA1 model showed stronger long-term-depression (LTD) for E-STDP on both excitatory and inhibitory neurons, and weaker long-term-potentiation (LTP) for E-STDP on the inhibitory neurons. For the other evolved hyper-parameters, the maximum weight for the Inh $\rightarrow$ Exc connection in the CA1 model is stronger than that in the SUB model (CA1: 0.54 ± 0.05, SUB: 0.16 ± 0.11, Wilcoxon's rank sum test, $p < 0.01$). The CA1 model also showed a trend of having smaller values for the time scale parameter T (CA1: 0.78 ± 0.35 s, SUB: 4.5 ± 3.29 s, Wilcoxon's rank sum test, $p = 0.056$) and the mean firing rate for the excitatory group (CA1: 2.28 ± 0.36 Hz, SUB: 5.19 ± 2.38 Hz, Wilcoxon's rank sum test, $p = 0.056$).

To make a quantitative comparison between the spatial representations emerged from the two modeled regions, we conducted spatial analyses on the excitatory neurons of both modeled region (Table I). These analyses were developed to interpret neural correlates of rodent navigation. We computed spatial information per spike [24], spatial sparsity [25], spatial selectivity [25], and spatial coherence [26]. As the excitatory neuron group was intended to model a larger population of neurons in the corresponding brain region, we

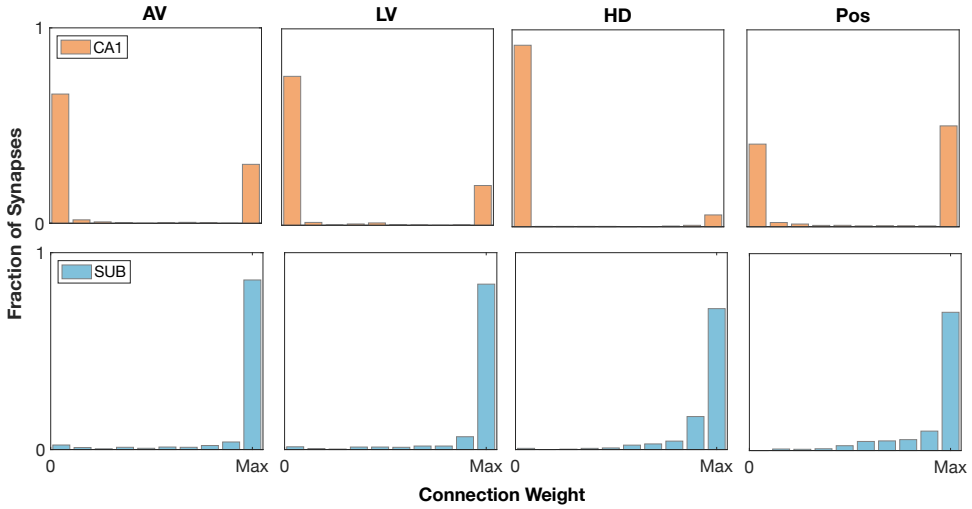

Fig. 5: Histograms of the connection weights from the input groups to the excitatory neuron groups. Weight values range from 0 to the maximum weight value, which was evolved by the EA. CA1 weights show more weights near 0 for AV, LV, and HD, and more weights near the maximum weight for Pos. In the SUB model, weight values of all four types of input all cluster near the maximum weight value.

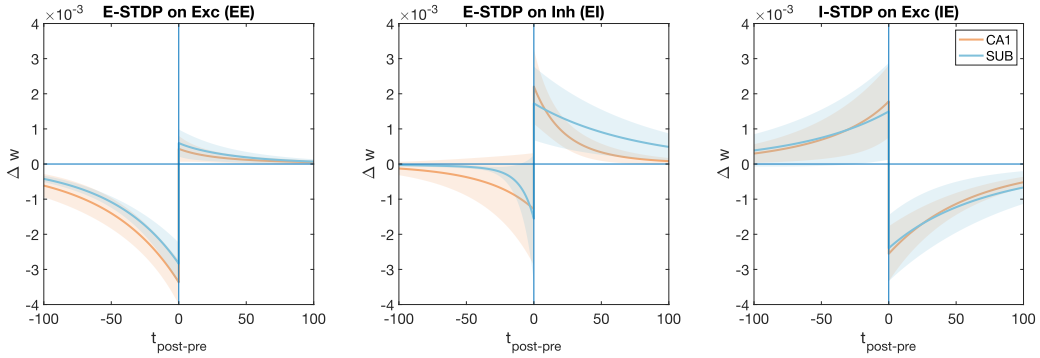

Fig. 6: Visualization of STDP curves used in the evolved and trained CA1 and SUB models. Solid lines show the mean, and shaded areas show the standard deviation of 5 evolutionary runs. CA1 model had slightly stronger LTD on the EE and EI connections, and weaker LTP on the EI connections. The I-STDP curve in both models had similar amplitude and time constant.

analyzed neurons from the entire group instead of only those explicitly matched to the experimentally observed neurons. Consistent with the experimentally observed neurons and other neurophysiological studies [3], SUB neurons showed higher firing rates, lower spatial information per spike, lower spatial selectivity, and lower spatial coherence than CA1 neurons (Wilcoxon's rank sum test, $p < 0.01$).

B. Population Vector Analysis

We conducted population vector analyses with positional reconstruction matrices to test whether the spatial representations of these simulated brain regions are similar to the rodent. The population activity in both models closely resembled that of the experimentally observed neurons. Computed with Equation 4, CA1 model units obtained a similarity score of 0.76 ± 0.01 and SUB model units obtained a score of 0.69 ± 0.01 (i.e., mean $\pm$ standard deviation).

Fig. 7 visualizes the positional reconstruction matrix for each model from a representative evolutionary run. Each value of the positional reconstruction matrix depicted the similarity of population activity in one location versus the activity in another location. Values on the diagonal line described the correlation of activity in the same location between odd and even trials. Both CA1 and SUB simulated neurons showed high correlation values on the diagonal line (median correlation value for CA1 averaged over 5 runs: 0.94 ± 0.01, for SUB: 0.96 ± 0.01), indicating that simulated neurons in both models reliably encoded locations. The two matrices also showed distinctive differences in off-diagonal values. Comparing the grids highlighted in red on both matrices, the SUB matrix had high correlation values around the diagonal in the grids while the CA1 matrix didn't show this pattern, indicating that the SUB model units had a stronger head-direction tuning. Additionally, for the grids highlighted in green, the SUB matrix

TABLE I: Spatial analyses on the model units (mean ± standard deviation) in the five evolutionary runs (sim) and the experimentally recorded neurons (recorded). Values in bold fonts showed greater values in comparison between CA1 and SUB neurons (Wilcoxon's rank sum test, $p < 0.01$).

SpatialMetrics	CA1 (sim)	SUB (sim)	CA1 (recorded)	SUB (recorded)
meanFR (Hz)	0.85 ± 0.87	**2.16 ± 2.00**	0.88 ± 1.42	**3.62 ± 4.23**
maxFR (Hz)	27.66 ± 18.78	**41.75 ± 33.35**	31.57 ± 14.91	**38.86 ± 21.35**
spatialIfo (bits)	**2.87 ± 1.04**	1.92 ± 0.69	**2.97 ± 1.19**	1.56 ± 1.21
sparsity	0.12 ± 0.08	**0.20 ± 0.10**	0.12 ± 0.13	**0.35 ± 0.25**
selectivity	**64.53 ± 74.53**	27.29 ± 21.47	**63.76 ± 50.79**	31.18 ± 38.84
spatialCoherence	**0.83 ± 0.05**	0.81 ± 0.05	0.48 ± 0.12	0.49 ± 0.14

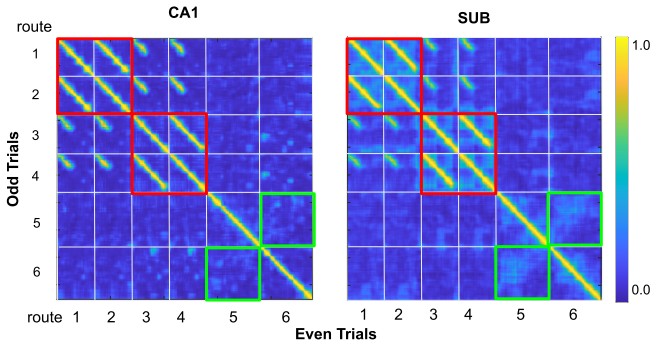

Fig. 7: Positional reconstruction matrices of the simulated CA1 and SUB populations. Mean activity of the even trials are correlated against that of the odd trials. Position bins for each route are shown on the axes. At each position bin, the color represents the correlation value. High values on the diagonal lines indicate that position along the route is inferred from population activity of the neurons. Grids highlighted in red and green show stronger head-direction and analogous tuning of SUB ensemble compared to CA1.

showed a square region of higher correlation values near the top left of the grids, which correspond to a higher correlation of population activity on the longer segments between Routes 5 and 6. These location pairs were spatially separated but shared the same head direction and analogous maze structure in the environment. These results indicate that the simulated SUB neurons had stronger head direction tuning and encoded analogous spaces more profoundly than the simulated CA1 neurons, which is consistent with the differences observed in the rodent CA1 and SUB [14].

C. Control Experiments

To verify the necessity of evolutionary algorithms and STDP learning in the optimization process, we ran the models in two additional conditions; one in which there was STDP but no EA, and another in which there was no STDP and no EA. In both conditions, we had 5 runs for each model, with each run including 15 individual networks initialized with random hyper-parameters. Similar to the fully evolved and trained models, models in the control experiments were evaluated with a fitness function (Equation 1), and the best performing network individual in each run was selected for population vector analysis.

In both these control cases, the performance of the SNNs was worse than evolving STDP-H parameters for 50 generations. In the "STDP no EA" condition, where each of the 15 networks went through the same training and testing procedure as the fully evolved models did but did not go through the evolutionary process, the CA1 model obtained an average similarity score of 0.46 ± 0.29 and the SUB model obtained an average similarity score of 0.60 ± 0.03. In the "no STDP no EA" condition, where each of the 15 networks was tested without being trained with STDP, the CA1 model obtained an average similarity score of 0.26 ± 0.36, and the SUB model obtained an average similarity score of 0.12 ± 0.28.

Taken together, these results show that STDP greatly improved the performance of the network, and that having multiple generations of evolutionary computation was necessary for finding the hyper-parameters that allow for higher resemblance of simulated neuronal activity to that of the modeled brain region. These control experiments suggest that parameter tuning through the evolutionary process and synaptic plasticity through STDP-H were necessary to replicate these brain regions. Similar results were reported when modeling the retrosplenial cortex (RSC) using this methodology [13].

D. Ablation Studies

To examine the effect of removing input streams on each modeled brain region, we conducted ablation studies using the fully evolved and trained networks. The ablation studies included lesions of connections from each of the input streams to both the excitatory and inhibitory neuron groups. Lesion models were created by loading the trained networks and removing the inter-group connections corresponding to the input stream(s). The lesion models were presented with the same input variables as the non-lesioned models, and the network activity was recorded. Population vector analysis was then performed on the lesion models to assess the impact of lesions of input streams.

Lesions had differential effects on model performance that reflect the spatial encoding of CA1 and SUB (Fig. 8). In the CA1 model, lesions of the positional input (Pos) had a strong impact on the performance of the network, while lesions of one of the three idiothetic inputs (AV, HD, and LV) did not have a strong effect on performance. Lesions of all three idiothetic inputs together (AV_HD_LV) had a stronger impact than individual lesions, but were weaker than lesions of Pos alone. Additionally, lesions of the head direction and positional inputs together (HD_Pos) brought the similarity score down

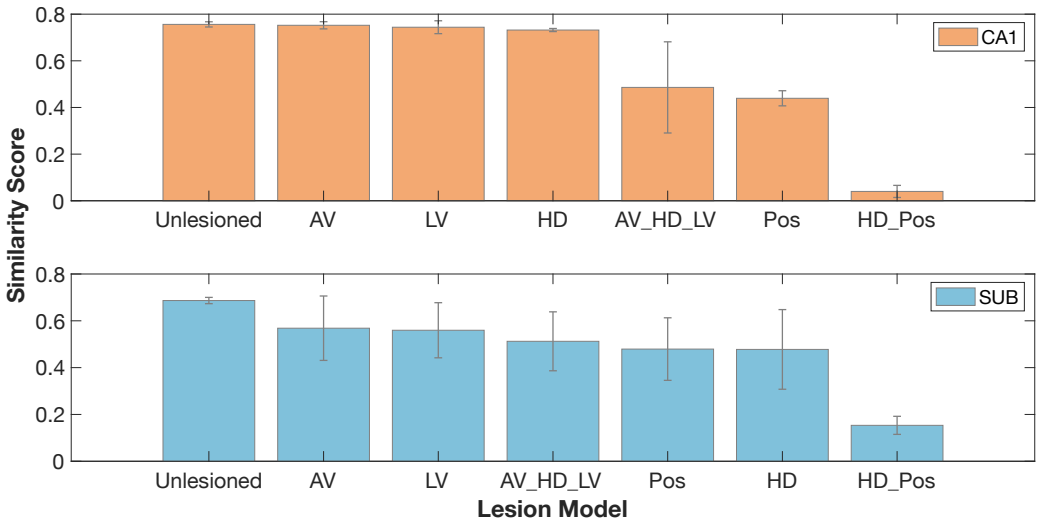

Fig. 8: Ablation studies: similarity scores of the unlesioned and lesioned models. Bars show the mean values and the error bars show standard deviation of scores obtained by 5 instances of each model. Lesions of the positional input (Pos) in the CA1 model had the strongest impact on the network performance compared to lesions of other single input streams. In the SUB model, lesions of all four types of input had a similar level of impact on the network performance.

to near 0. In contrast, lesions of any input stream to the SUB had a moderate impact on network performance. Similar to the CA1 model, lesions of the head direction and positional inputs together (HD_Pos) in the SUB model greatly decreased the similarity score. Taken together, these ablation studies further support that the CA1 is more place specific and the SUB is more driven by inputs related to action or movement.

IV. Discussion

The spiking neural network modeling framework presented here captured the differing spatial responses of hippocampal CA1 and the SUB through unsupervised learning, via STDP-H, and evolutionary algorithms (EAs). The resulting networks show highly place-specific responses in CA1 neurons and the emergence of pattern recurrence in the spatially specific firing of SUB neurons. These differing functional responses were reflected in the STDP-H parameters and the weight distributions of the simulated spiking neural networks (SNNs). Moreover, the present simulations make testable experimental predictions for the plasticity and connectivity in these brain areas.

The evolutionary algorithm automated the design of SNNs by indirect encoding of network learning parameters. This approach had been shown in a previous study to successfully replicate neural dynamics observed in the retrosplenial cortex (RSC) as rodents traverse a W-shaped maze [13]. In the present work, we extended the approach to model two other regions that are important to spatial navigation: hippocampal CA1 and the SUB. Using data recorded in the two brain regions when rats performed the same navigational task in the same environment allowed us to compare our two models directly.

With the same input representations, the EAs selected different STDP-H learning parameters for the two SNN models, which led to different connection weight distributions. STDP-H parameters in the CA1 models had more LTD than in SUB, which led to a strong pruning effect in the CA1 excitatory group. In contrast, synapses connecting the AV, LV, and HD input groups with the SUB excitatory groups had larger connection weights than in the CA1 model, suggesting stronger vestibular inputs to the SUB model, which is consistent with neurophysiological observations [20], [27].

Different distributions of connection weights in turn allowed for divergent spatial representations to emerge in the network models. These spatial representations, as analyzed through firing rate distributions, firing rate map visualizations, classic spatial metrics including spatial information, sparsity, selectivity, and spatial coherence, were consistent with those observed in the experimentally recorded neurons. The network models, though simplified in terms of the types of input information and network sizes, generated neural dynamics resembling those observed in the real neural circuits. It should be noted that although only a subset of simulated neurons were optimized to match with recorded neurons, all neurons in the simulated neuron groups were included in the analyses and showed consistent response properties within the group. This suggests that our modeling approach allowed for generalization of learned firing patterns to unobserved data.

Results of the control experiments underscore the importance of combining both STDP and evolutionary computation in the modeling framework. By evolving the learning parameters, the search space is dramatically reduced, as compared to directly evolving weights or using a method such as back-propagation. This study further suggests a functional role for STDP-H. The result is a viable SNN that can be used for a range of simulation studies. The success in modeling CA1, SUB and RSC [13] suggests that the approach may be a

general-purpose means to building SNNs.

In the ablation studies, we removed one or more input streams from the fully evolved and trained networks. Lesions of positional input to the CA1 model had a stronger impact on the network performance than the other three input streams, suggesting that spatial representations in CA1 are more reliant on the CA3 input to CA1 than self-motion signals. In the SUB model, lesions of any one of the four input streams had a similar level of impact on the network performance, suggesting that the SUB model utilized different input information more equally.

In addition to showing single place fields as CA1 neurons do, SUB neurons often encode multiple locations that share certain spatial features in a triple-T maze environment [14]. These representations may require an integration of idiothetic information as well as positional information. In both models, a significant drop in the similarity score was observed when two or more input streams were lesioned together, suggesting a conjunctive coding of multiple input variables in the CA1 and SUB models, which coincides with the evidence that CA1 and SUB neurons are encoding multiple types of signals [28], [29].

The presented modeling approach could be extended to include multiple brain regions to investigate how they interact. In future studies, we will integrate findings in this work and link together the CA1 and SUB models. As neurophysiological studies suggest, SUB receives a strong input from CA1, and SUB also sends backward projections to CA1 [20], [30]. Following these findings, we can investigate how the interaction between the two regions work together during navigation by connecting the two models and examining how information is integrated between these brain regions.

Acknowledgment

This material is based upon work supported by the United States Air Force Award #FA9550-19-1-0306. Any opinions, findings and conclusions or recommendations expressed in this material are those of the author(s) and do not necessarily reflect the views of the United States Air Force.

References

[1] R. G. Morris, F. Schenk, F. Tweedie, and L. E. Jarrard, "Ibotenate Lesions of Hippocampus and/or Subiculum: Dissociating Components of Allocentric Spatial Learning," *Eur. J. Neurosci.*, vol. 2, no. 12, pp. 1016–1028, 1990.

[2] J. O'Keefe and J. Dostrovsky, "The hippocampus as a spatial map. Preliminary evidence from unit activity in the freely-moving rat," *Brain Res.*, vol. 34, no. 1, pp. 171–175, nov 1971.

[3] P. E. Sharp and C. Green, "Spatial correlates of firing patterns of single cells in the subiculum of the freely moving rat," *J. Neurosci.*, vol. 14, no. 4, pp. 2339–2356, 1994.

[4] M. Wilson and B. McNaughton, "Dynamics of the hippocampal ensemble code for space," *Science*, vol. 261, no. 5124, pp. 1055–1058, 1993.

[5] O. Potvin, F. Y. Doré, and S. Goulet, "Contributions of the dorsal hippocampus and the dorsal subiculum to processing of idiothetic information and spatial memory," *Neurobiol. Learn. Mem.*, vol. 87, no. 4, pp. 669–678, may 2007.

[6] J. M. Olson, K. Tongprasearth, and D. A. Nitz, "Subiculum neurons map the current axis of travel," *Nat. Neurosci.*, vol. 20, no. 2, pp. 170–172, feb 2017.

[7] A. Arleo and W. Gerstner, "Spatial cognition and neuro-mimetic navigation: A model of hippocampal place cell activity," *Biol. Cybern.*, vol. 83, no. 3, pp. 287–299, 2000.

[8] N. Burgess and J. O'Keefe, "Models of place and grid cell firing and theta rhythmicity," *Curr. Opin. Neurobiol.*, vol. 21, no. 5, pp. 734–744, oct 2011.

[9] M. Tsodyks and T. Sejnowski, "Associative memory and hippocampal place cells," Tech. Rep., 1995.

[10] Q. Xu, J. Peng, J. Shen, H. Tang, and G. Pan, "Deep covdensesnn: A hierarchical event-driven dynamic framework with spiking neurons in noisy environment," *Neural Networks*, vol. 121, pp. 512–519, 2020.

[11] N. K. Kasabov, "Neucube: A spiking neural network architecture for mapping, learning and understanding of spatio-temporal brain data," *Neural Networks*, vol. 52, pp. 62–76, 2014.

[12] P. Diehl and M. Cook, "Unsupervised learning of digit recognition using spike-timing-dependent plasticity," *Frontiers in Computational Neuroscience*, vol. 9, p. 99, 2015.

[13] E. L. Rounds, A. S. Alexander, D. A. Nitz, and J. L. Krichmar, "Conjunctive Coding in an Evolved Spiking Model of Retrosplenial Cortex," *Behav. Neurosci.*, 2018.

[14] J. M. Olson, A. B. Johnson, L. Chang, E. L. Tao, and D. A. Nitz, "Complementary Maps for Location and Environmental Structure in CA1 and Subiculum," *bioRxiv*, p. 2021.02.01.428537, feb 2021.

[15] T. S. Chou, H. J. Kashyap, J. Xing, S. Listopad, E. L. Rounds, M. Beyeler, N. Dutt, and J. L. Krichmar, "CARLsim 4: An Open Source Library for Large Scale, Biologically Detailed Spiking Neural Network Simulation using Heterogeneous Clusters," *Proc. Int. Jt. Conf. Neural Networks*, vol. 2018-July, pp. 1158–1165, 2018.

[16] S. Luke, "Ecj then and now," *Proceedings of the Genetic and Evolutionary Computation Conference Companion*, p. 1223–1230, 2017. [Online]. Available: https://doi.org/10.1145/3067695.3082467

[17] E. M. Izhikevich, "Simple Model of Spiking Neuron," *IEEE Trans. Neural Networks*, vol. 14, no. 6, pp. 1569–1572, 2003.

[18] J. K. Leutgeb, S. Leutgeb, M.-B. Moser, and E. I. Moser, "Pattern Separation in the Dentate Gyrus and CA3 of the Hippocampus," *Science (80-.).*, vol. 315, no. 5814, pp. 961 LP – 966, feb 2007.

[19] E. Kropff, J. E. Carmichael, M.-B. Moser, and E. I. Moser, "Speed cells in the medial entorhinal cortex," *Nature*, vol. 523, no. 7561, pp. 419–424, 2015.

[20] S. O'Mara, "The subiculum: what it does, what it might do, and what neuroanatomy has yet to tell us," *J. Anat.*, vol. 207, no. 3, pp. 271–282, sep 2005.

[21] B. E. Frost, S. K. Martin, M. Cafalchio, M. N. Islam, J. P. Aggleton, and S. M. O'Mara, "Anterior thalamic function is required for spatial coding in the subiculum and is necessary for spatial memory," 2020.

[22] K. D. Carlson, M. Richert, N. Dutt, and J. L. Krichmar, "Biologically plausible models of homeostasis and stdp: Stability and learning in spiking neural networks," pp. 1–8, 2013.

[23] S. L. Cowen and D. A. Nitz, "Repeating firing fields of CA1 neurons shift forward in response to increasing angular velocity," *J. Neurosci.*, vol. 34, no. 1, pp. 232–241, 2014.

[24] W. E. Skaggs, B. L. McNaughton, K. M. Gothard, and E. J. Markus, "An Information-Theoretic Approach to Deciphering the Hippocampal Code," *Proceedings of the 5th International Conference on Neural Information Processing Systems*, 1993.

[25] W. E. Skaggs, B. L. McNaughton, M. A. Wilson, and C. A. Barnes, "Theta phase precession in hippocampal neuronal populations and the compression of temporal sequences," *Hippocampus*, vol. 6, no. 2, pp. 149–172, jan 1996.

[26] J. L. Kubie, R. U. Muller, and E. Bostock, "Spatial Firing Properties of Hippocampal Theta Cells," Tech. Rep. 4, 1990.

[27] G. V. Allen and D. A. Hopkins, "Mamillary body in the rat: Topography and synaptology of projections from the subicular complex, prefrontal cortex, and midbrain tegmentum," *J. Comp. Neurol.*, vol. 286, no. 3, pp. 311–336, 1989.

[28] R. U. Muller, E. Bostock, J. S. Taube, and J. L. Kubie, "On the directional firing properties of hippocampal place cells," *J. Neurosci.*, vol. 14, no. 12, pp. 7235–7251, 1994.

[29] T. Kitanishi, R. Umaba, and K. Mizuseki, "Robust information routing by dorsal subiculum neurons," *bioRxiv*, 2020.

[30] X. Xu, Y. Sun, T. C. Holmes, and A. J. López, "Noncanonical connections between the subiculum and hippocampal ca1," *Journal of Comparative Neurology*, vol. 524, no. 17, pp. 3666–3673, 2016.